New Opportunities for Lanthanide Luminescence

Jean-Claude G. Bünzli*, Steve Comby, Anne-Sophie Chauvin, Caroline D. B. Vandevyver

(Laboratory of Lanthanide Supramolecular Chemistry, École Polytechnique Fédérale de Lausanne, BCH 1402, CH-1015, Lausanne, Switzerland)

Abstract: Trivalent lanthanide ions display fascinating optical properties. The discovery of the corresponding elements and their first industrial uses were intimately linked to their optical properties. This relationship has been kept alive until today when many high-technology applications of lanthanide-containing materials such as energy-saving lighting devices, displays, optical fibers and amplifiers, lasers, responsive luminescent stains for biomedical analyses and in cellulo sensing and imaging, heavily rely on the brilliant and pure-color emission of lanthanide ions. In this review we first outlined the basics of lanthanide luminescence with emphasis on f-f transitions, the sensitization mechanisms, and the assessment of the luminescence efficiency of lanthanide-containing emissive molecular edifices. Emphasis was then put on two fast developing aspects of lanthanide luminescence: materials for telecommunications and light emitting diodes, and biomedical imaging and sensing. Recent advances in NIR-emitting materials for plastic amplifiers and waveguides were described, together with the main solutions brought by researchers to minimize non-radiative deactivation of excited states. The demonstration in 1999 that erbium tris(8-hydroxyquinolinate) displayed a bright green emission suitable for organic light emitting diodes (OLEDs) was followed by realizing that in OLEDs, 25% of the excitation energy leads to singlet states and 75% to triplet states. Since lanthanide ions are good triplet quenchers, they now also play a key role in the development of these lighting devices. Luminescence analyses of biological molecules are among the most sensitive analytical techniques known. The long lifetime of the lanthanide excited states allows time-resolved spectroscopy to be used, suppressing the sample autofluorescence and reaching very low detection limits. Not only visible lanthanide sensors are now ubiquitously provided in medical diagnosis and in cell imaging, but the feasibility of using NIR emission of ions such as Yb^{III} is now being tested because of deeper penetration in biological tissues.

Key words: lanthanide luminescence; sensitization; near infrared; telecommunications; organic light emitting diode (OLED); time-resolved luminescence; in cellulo sensing; cell imaging; rare earths

CLC number: O482.3; O614.33   **Document code**: A   **Article ID**: 1002 - 0721(2007)03 - 0257 - 18

According to the International Union of Pure and Applied Chemistry (IUPAC) recommendations (1968), *lanthanides* include elements 58 (Ce) to 71 (Lu), while the whole series from La (57) to Lu (71) should be called *lanthanoids*; when Sc (21) and Y (39) are added to the latter, then the resulting 17 elements should be termed rare earths. In practice, however, *lanthanoids* is rarely used, to the benefit of lantha-

nides. The fascinating story of lanthanide elements started at the end of the 18th century when Carl Axel Arrhenius, an artillery lieutenant of the Swedish army, found a curious black mineral in a feldspath quarry near Ytterby in 1787[1,2]. The latter is located on a small island (Vaxholm) governing the entrance of Stockholm harbor. The mineral was called "Ytterby's tungsten" because in Swedish "tung sten" means

"heavy stone" and its analysis in 1788 by Geier B R, a mineralogist located in Stockholm, revealed a new mineral. Due to vacancies at the chemistry department of Stockholm University, chemical analysis was only carried out in 1794 by Johan Gadolin, a professor at Åbo (today Turku, Finland) University, who identified a new element which he named yttrium[3,4]. The next 15 rare earth elements were discovered between 1803 (Ce) and 1907 (Lu) by outstanding scientists (Berzelius J J, Mosander C G, Galissard de Marignac J C, Cleve P T, LeCoq de Boisbaudran P E, Demarçay E A, Urbain G among others) while the last one, artificial Pm, had to wait its synthesis until 1947.

The first industrial application of a lanthanide element was proposed in 1891 by the extraordinary scientist and entrepreneur Carl Auer von Welsbach, who studied chemistry in Vienna and then in Heidelberg with Bunsen R W. Just after completing his PhD degree, he discovered two lanthanide elements in 1885, Pr and Nd. The same year he filed a patent for electric bulbs containing Os and W filaments. But electricity was not readily available in those times and, as an alternative, Auer von Welsbach proposed the so-called *Auer mantle* for gas lighting in 1891. The mantle is made up of 99% thorium oxide and 1% cerium oxide; more than five billions were sold until 1935 and the company founded by Auer von Welsbach, *Treibacher Chemische Werke*, which also manufactured flint stones and *Mishmetal* (an alloy of 30% iron and 70% of a mixture of La, Ce, Nd, and Sm), is still producing rare earth materials nowadays. The other company founded in 1906 by Auer von Welsbach for the production of light bulbs, Osram, developed into a large multinational business which presently employs over 38000 collaborators.

The lanthanides are unique among the elements, except for the actinides, in resembling each other so markedly[5,6]. This is easily explained by the electronic configuration of the atoms and their derived ions, which essentially exist in the trivalent state Ln^{III} ($[Xe]4f^n$, $n = 0 \sim 14$) in aqueous solutions. The shielding of the 4f orbitals by the filled $5p^6 6s^2$ sub-shells results in special spectroscopic properties with parity-forbidden 4f-4f transitions having very low molar absorption coefficients (< 10 M$^{-1} \cdot$cm^{-1}, but very often < 1 M$^{-1} \cdot$cm^{-1}) and characteristic narrow-line emission, mostly in the visible and near infrared ranges. Luminescence has been instrumental in the discovery of several lanthanide elements and in turn, these elements have always played a prominent role in lighting and light conversion technologies (Auer mantles, incandescent lamps, lasers) and more recently in cathode-ray[7]

and plasma[8] displays, and light-emitting diodes[9].

In the 1980's, it was realized that the peculiar luminescent properties of the lanthanide ions could be of great help in the analysis of environmental and biological samples[10,11] and this led to most interesting developments which have stirred a vast interest for the coordination chemistry of these ions. Presently, attention focuses on several applications of luminescent lanthanide ions[12,13]: (1) their continuing use in lighting industry for the engineering of lamp and display phosphors[8], (2) their ability to provide electroluminescent materials for organic light-emitting diodes as well as optical fibers and amplifiers for telecommunications[14], (3) their potential in the design of luminescent liquid crystals[15], and (4) their capacity to yield functional complexes for biological assays[16,17] and medical imaging purposes[18].

After a short summary of lanthanide luminescent properties, the present feature article focuses on two applications of trivalent lanthanide luminescence which sustain a particularly large development, materials for telecommunications, and luminescent probes for bioanalyses. This contribution however does not intend to provide a full coverage of the relevant bibliography.

1 Lanthanide Luminescence

The spectroscopic properties of trivalent lanthanide ions are fascinating in that their $[Xe]4f^n$ electronic configuration generates numerous electronic levels, up to 3432 for Gd^{III} for instance, as one easily calculates from the combinatorial formula (1) where l is 3 for f-electrons.

$$\frac{(4l+2)!}{n!\,(4l+2-n)!} \tag{1}$$

The trivalent lanthanide ions may be implied in three types of electronic transitions:

(1) Charge transfer transitions[19,20]

Both ligand-to-metal (LMCT) and metal-to-ligand (MLCT) transitions are allowed by Laporte's selection rule. Their energy is usually very large, so that they appear in the UV above 40000 cm^{-1} ($\lambda < 250$ nm), except for the ions which may be relatively easy either reduced to their $+2$ state (Sm^{III}, Eu^{III}, Tm^{III}, Yb^{III}), or oxidized to their $+4$ state (Ce^{III}, Pr^{III}, Tb^{III}). In these cases, the broad charge transfer transitions may occur at energies as low as 30000 cm^{-1} ($\lambda \approx 330$ nm). For the other ions, any assignment of LMCT transition below 40000 cm^{-1} must be considered as being dubious. From a practical viewpoint, LMCT transitions are used in lamp phosphors to pump energy into Eu^{III} or Tb^{III}, for instance.

(2) 4f-5d transitions[21]

They correspond to the promotion of a 4f electron into the 5d sub-shell and are also allowed by the parity rule, resulting in sizeable oscillator strengths with absorption coefficients in the range $10^2 \sim 10^3$ M$^{-1}\cdot$cm^{-1}, that is, comparable to those of the charge transfer transitions. Their energy depends largely upon the metal environment because 5d orbitals are external and they interact directly with ligand orbitals; however, these transitions are also quite energetic and only those of Ce^{III}, Pr^{III} and Tb^{III} are commonly observed below 45000 cm^{-1} ($\lambda < 220$ nm).

(3) f-f transitions

The sharp f-f transitions, involve a rearrangement of the electrons in the 4f sub-shell and are therefore polarity forbidden, which explains their faint intensities. These transitions are quite narrow and the barycenter of the ligand-field split bands is fairly insensitive to the metal ion environment. As a consequence, they are easily recognizable and therefore lanthanide ions are ideal candidates for optical probes.

Most of the trivalent lanthanide ions are luminescent (Fig. 1), either fluorescent (Pr^{III}, Nd^{III}, Ho^{III}, Er^{III}, Yb^{III}) or phosphorescent (Sm^{III}, Eu^{III}, Gd^{III}, Tb^{III}, Dy^{III}, Tm^{III}). Some ions, such as Pr^{III}, present both fluorescent (i.e. with $\Delta S = 0$) and phosphorescent ($\Delta S > 0$) transitions. The emission of the Ln^{III} ions covers the entire spectrum (0.3 $\sim$ 3 μm), from UV(Gd^{III}) to visible (e.g., blue Tm^{III}, green Tb^{III}, orange Sm^{III}, or red Eu^{III}), and near-infrared (NIR) spectral ranges (e.g., Pr^{III}, Nd^{III}, Er^{III}, Yb^{III}, see Fig. 2)[22]. The Stokes' shifts are very small when the ions are excited through f-f transitions since the rearrangement of the electrons in the 4f sub-shell does not lead to much change in the chemical bond lengths, contrary to what is observed with organic compounds or d-transition metal
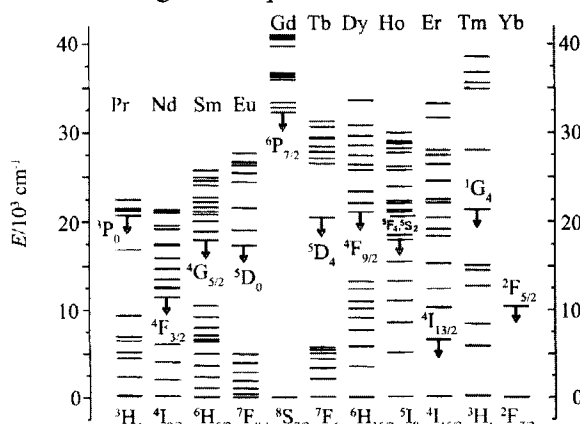

Fig. 1   Partial energy diagrams of lanthanide trivalent ions (except La, Ce, Pm, Lu). Labels are given for ground states and for one of the most luminescent excited states (with a few exceptions, several excited states are usually luminescent for a given ion)
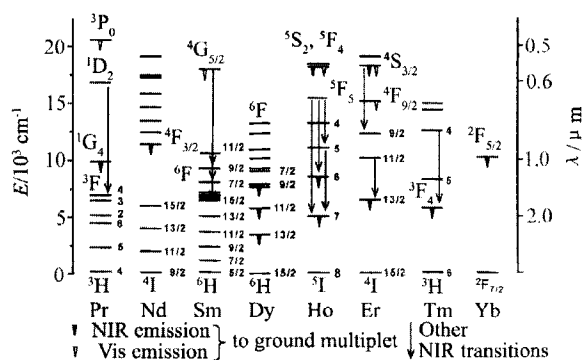

Fig. 2   Partial energy diagrams of NIR-emitting trivalent lanthanide ions. Energies are for aquo-ions[22]

ions. Two ions, La^{III} and Lu^{III}, have no f-f transitions and are not luminescent, while Ce^{III} displays an intense d-f emission which can be tuned from 290 to 500 nm. Ions in other oxidation states are also luminescent, e.g., Sm^{II} (sharp-band emission), Eu^{II} and Yb^{II} (broad band emission), but here we restrict ourselves to trivalent ions.

1.1   Sensitization processes

To overcome the problem of weak f-f oscillator strengths when exciting the luminescent lanthanide ions, energy is often transferred from the surroundings of the metal ion (either an inorganic matrix or an organic ligand) in a three-step mechanism: absorption of light by the surroundings, transfer onto the lanthanide ion, and emission of light. The overall process is quite complex and involves several mechanisms and energy levels. Its optimization is crucial to the overall luminescence yield that can be obtained. In addition to providing an efficient path for the excitation of lanthanide ions, this sensitization process has also the advantage that now the "Stokes' shifts" are very large, which allows an easy spectral separation of the remaining matrix luminescence from the metal ion emission. Modeling of this complex process is now at hand for coordination compounds. It implies (1) calculation of the ligand excited singlet and triplet states, (2) determination of which levels are likely to be implied using selection rules and energy-match criteria, (3) identifying the operating mechanisms (exchange, dipole-dipole, dipole-multipole), (4) writing the rate equation for all likely energy migration paths, and (5) solving these equations[23~25].

The main energy transfer and de-activation paths are sketched on Fig. 3 for the special case of a molecular lanthanide-containing complex. Although very often the ^{1}S* (ligand)-^{3}T* (ligand)-4f* path is predominant, particularly for Eu^{III} and Tb^{III}, this is by no means the only energy conduit within the molecule
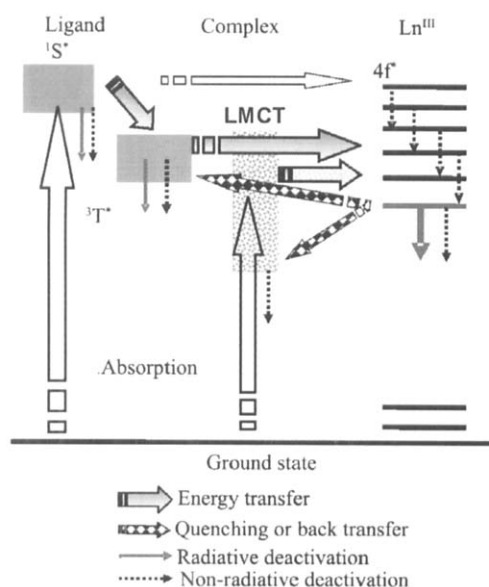
Fig. 3   Schematic energy diagram showing the main energy transfer paths and de-activation processes

and there are several examples of $^1S^*$ (ligand)-4f* direct transfers[26], of sensitization through either d-transition metal levels, e.g., Cr^{III} (^2E)-$Eu(^5D_0)$[27], or ^3MLCT[28], e.g., $Ru^{II}(^3MLCT)$-Yb^{III} $(^2F_{5/2})$[29], or of excitation of a given Ln^{III} ion by another one, one classical example being the sensitization of Er^{III} through Yb^{III} or Ce^{III}[30]. Implication of $4f^{n-1}5d^1$ and intraligand charge transfer states (ILCT) in the energy transfer process has also been invoked[31~33]. In some instances, generation of the ligand $^3T^*$ state goes through an intramolecular electron-transfer step made possible thanks to coordination of the 4f-element[34].

One point to be stressed here is the role of LM-CT states which are only of importance for easily reducible Ln^{III} ions: when they lie at high energy enough (typically > 24000 cm^{-1} for Eu^{III} complexes), they may act as antennae and transfer energy onto the metal ion; on the other hand, when their energy is low, they are very efficient quenchers of the Ln^{III} luminescence[35,36]. Since the latter process is thermally activated, a drop in the lifetime of the quenched Ln^{III} state with increasing temperature is diagnostic of its presence. Generally speaking, back energy transfer from the excited metal ion onto the ligand, an undesirable process, is also inducing a drop in lifetime with increasing temperature, as are vibration quenching mechanisms.

1.2   Assessing the luminescence efficiency

The synthetic chemist has to meet several requirements in order to come up with a highly luminescent molecule or material which, of course, depend

on the searched for property. In the case of photoluminescence, the parameter of interest is the product of the overall quantum yield Q_{Ln}^L by the overlap integral between the absorption spectrum A (λ) of the lanthanide compound and the emission spectrum $E_{exc}(\lambda)$ of the excitation source:

$$\Phi_{lum} = Q_{Ln}^L \times \int A\,(\lambda) \cdot E_{exc}(\lambda) \cdot S(\lambda) \qquad (2a)$$

where the integration is made on the spectral range in which the excitation is effective (i.e., taking into account the slit function of the spectrometer, $S(\lambda)$). For comparison purposes between compounds, this overall efficiency (Φ_{lum}) can be approximated by the product of Q_{Ln}^L by the molar absorbance at the excitation wavelength, ε_λ:

$$\Phi_{lum} \approx Q_{Ln}^L \times \varepsilon_\lambda \qquad (2b)$$

In the case of sensitization through the ligand levels, the overall quantum yield of a lanthanide-containing molecular edifice is given by

$$Q_{Ln}^L = \eta_{sens} \cdot Q_{Ln}^{Ln} = \eta_{sens} \cdot \frac{\tau_{obs}}{\tau_{rad}} \qquad (3)$$

whereby Q_{Ln}^L and Q_{Ln}^{Ln} are the overall and intrinsic quantum yields resulting from indirect and direct excitation, respectively, while η_{sens} represents the efficacy with which electromagnetic energy is transferred from the surroundings onto the metal ion; τ_{obs} is the experimental lifetime of the metal excited state (measured upon direct excitation) and τ_{rad} is its radiative lifetime. The intrinsic quantum yield Q_{Ln}^{Ln} essentially depends on the energy gap between the lowest lying excited (emissive) state of the metal ion and the highest sub-level of its ground multiplet. The smaller this gap the easier is its closing by non-radiative de-activation processes, for instance via vibrations of bound ligands, particularly those with high energy vibrators such as O - H, N - H, or C - H. The latter phenomenon is more important if the energy difference ΔE between the emitting level and the highest spin-orbit sub-level of the Ln^{III} ground state is small; this is the so-called "energy gap law"; as a first approximation, one may say that radiative de-excitation will compete efficiently with multi-phonon quenching processes if ΔE is equal to or larger than six quanta of the highest energy vibration present in the system.

If only one, simplified energy transfer scheme is taken into account, namely $^1S^* \rightarrow ^3T^* \rightarrow 4f^*$, Eq.(3) can be developed as follows:

$$Q_{Ln}^L = \eta_{isc} \cdot \eta_{et} \cdot Q_{Ln}^{Ln} \qquad (4)$$

with η_{isc} representing the efficacy of the intersystem crossing process and η_{et} the effectiveness of the $^3T \rightarrow 4f^*$ transfer. When excitation of $^3T^*$ leads to a relatively large expansion of the Ln-L distance, energy

transfer occurs as long as the higher vibrational levels of the triplet state are populated, that is the transfer stops when the lowest vibrational level is reached and triplet state phosphorescence takes over. On the other hand, if the Ln-L expansion is small, transfer is feasible as long as the triplet state is populated. If the rate constant of the transfer is large with respect to both radiative and non-radiative de-activation of $^3T^*$, the transfer then becomes very efficient ($\eta_{sens} \approx 1$, Eq. (3)). In order to compare the ability of chromophores to sensitize Ln^{III} luminescence, both the overall and intrinsic quantum yields have to be determined experimentally. If general procedures for measuring Q_{Ln}^L are well known for both solutions[37] and solid state samples[38], measurement of Q_{Ln}^{Ln} is not always easy in view of the very small absorption coefficients of the f-f transitions. This quantity can in principle be estimated differently, from the radiative lifetime. The latter is related to Einstein's expression for the rate of spontaneous emission A from an initial state $| \Psi J >$ characterized by a J quantum number to a final state $| \Psi'J' >$[39]:

$$A (\Psi J, \Psi'J') = \frac{64\pi^2}{3h} \cdot \frac{\tilde{v}_0^3}{(2J+1)} \cdot$$
$$\left[\frac{n(n^2+2)^2}{9} \cdot P_{ed} + n^3 \cdot P_{md} \right] \quad (5)$$

where $\tilde{v}_0$ is the energy of the transition, n the refractive index, h is Planck's constant (6.63×10^{-27} erg $\cdot$ s), and P_{ed} and P_{md} are the oscillator strengths of the electric dipole and magnetic dipole contributions to the transitions. According to Judd-Ofelt theory:

$$P_{ed} = e^2 \sum_{\lambda = 2, 4, 6} \Omega_\lambda | <J \| U^\lambda \| J' > |^2 \quad (6)$$

with Ω_λ representing the Judd-Ofelt parameters[40, 41] and U^λ doubly reduced matrix elements which are tabulated[42]. The magnetic dipole contribution can be calculated from:

$$P_{md} = \frac{4\pi^2 e^2 h}{3m^2 c^2} \cdot \frac{\tilde{v}_0^3}{(2J+1)} \cdot | <J \| L +2S \| J' > |^2 \quad (7)$$

where $L +2S$ is the spin-orbit operator which can be evaluated according to published methods[43], and e, m, c have their usual meaning. Then if the excited state $| \Psi J>$ relaxes to several different states $| \Psi'J' >$, the radiative lifetime τ^{rad} is equal to:

$$\tau^{rad} = \frac{1}{\sum_{J'} A (\Psi J, \Psi'J')} \quad (8)$$

The radiative lifetime can therefore be estimated from the spectral intensity with the help of Eqs. (5) ~ (8). Except for the special case of Eu^{III} for which a convenient simplified equation can be derived because one transition $^5D_0 \rightarrow {}^7F_1$ has a pure magnetic origin[44], this calculation is not trivial and large errors can occur,

including those pertaining to the hypotheses made. In particular it has been assumed that the emitting and receiving levels are really $(2J + 1)$-fold degenerate or, if split by crystal field effects, that all the sublevels are equally populated. This is obviously not true and in the case of Er^{III} this may lead to errors up to 20%. If the absorption spectrum corresponding to an emission spectrum is known however, which may be the case when the luminescence transitions terminate onto the ground level, the radiative lifetime is equal to Eq. (9) (Eqs. (5) ~ (9) are given within the frame of the cgs-esu unit system. Oscillator strengths are therefore expressed in esu^2 $\cdot$cm^2 = debye^2 while Ω_λ parameters are in cm^2):

$$\frac{1}{\tau_{rad}} = 2303 \cdot \frac{8\pi cn^2\tilde{v}_0^2}{N_A} \cdot \frac{(2J'+1)}{(2J+1)} \cdot \int \varepsilon(\tilde{v})d\tilde{v} \quad (9)$$

c is the speed of light *in vacuo* (in cm $\cdot$s^{-1}), $\tilde{v}_0$ is the energy of the transition in cm^{-1}, n is the refractive index of the medium, N_A is Avogadro's number, $\varepsilon(\tilde{v})$ is the absorption spectrum of transition in M$^{-1}\cdot$cm^{-1} vs. wavenumbers[44]. In the case of Eu^{III} the simplified equation is:

$$k_r = \frac{1}{\tau_r} = A_{MD,0} n^3 (\frac{I_{tot}}{I_{MD}}) \quad (10)$$

in which $A_{MD,0} = 14.65$ s^{-1} is the spontaneous emission probability of the $^5D_0 \rightarrow {}^7F_1$ transition and I_{tot}/I_{MD} the ratio of the integrated total emission from the $^5D_0 \rightarrow {}^7F_J$ transitions ($J = 0 \sim 6$) to the area of the $^5D_0 \rightarrow {}^7F_1$ transition. The intrinsic quantum yield is then simply equal to the ratio of the observed lifetime to the radiative lifetime calculated with Eq.(10):

$$Q_{Eu}^{Eu} = \frac{\tau_{obs}}{\tau_r} \quad (11)$$

It is to be stressed here that the radiative lifetime is associated with a given excited electronic level and contrary to what is often believed, it differs from one compound to another.

1.3 Designing molecular luminescent edifices

In designing a convenient chemical environment for a luminescent lanthanide ion, the chemists have to take into account three main requirements. The first one is a chemical constraint in that the coordination cavity should provide enough donor atoms to saturate the coordination number requirement of the Ln^{III} ion as well as a large bonding strength ensuring a good thermodynamic stability[45] and, possibly also kinetic inertness. The second requirement pertains to the efficiency of the sensitization process, i.e., the energy level scheme of the ligands should be such that it maximizes the energy transfer path (η_{sens}). This aspect

is fairly well mastered nowadays[13,46]. The third requirement deals with preventing non-radiative de-activation processes. This is by far a more delicate problem, which is particularly acute for NIR-emitting ions, since it means eliminating high energy vibrations from the first AND second coordination spheres; for instance, a recent estimate led to the conclusion that in the case of Er^{III} luminescence, the chemical environment of the emitting ion should be devoid of C-H vibrators up to distances ranging between 2.0 and 3.0 nm for the radiative rate constant to be larger than the non-radiative one[47]. Finally there might be additional prerequisites depending on the specific system designed, for instance with respect to its stability in biological fluids if an analytical sensor is tailored for bio-analyses. In the latter case, a quantum yield of about 10 % (Eu - , Tb-probes) is needed to yield sensitive enough analyses and the corresponding complex should have an excitation wavelength close to one of the readily available laser lines or newly developed light emitting diodes.

To meet these requirements, several imaginative synthetic strategies have been developed during the last decades, which include (1) linear polydentate and multifunctional ligands such as polyaminocarboxylates[48,49], β-diketonates[50], and acyclic Schiff base derivatives[51], (2) macrocyclic receptors[52] among which porphyrins[53,46], derivatized calixarenes[54], and pendant-arm fitted cyclens[52] are the most investigated, and (3) podates and self-assembled structures[55,56].

2 Materials for Telecommunications and Light-Emitting Diodes

This field has seen a tremendous upsurge of interest with the development of optical fibers for telecommunications and of light emitting diodes for economical lighting, a welcome effort in view of the worldwide energy crisis.

2.1 Amplifiers and waveguides for telecommunications[57,46]

In optical systems for telecommunications, light carries information between several users. Optical links consisting in single-mode silica optical fibers have the ability of providing high-bandwidth and long-distance communication. The manipulation of the optical signals on a local scale requires splitters, couplers, multiplexers, de-multiplexers, and amplifiers. These devices are easy to make and can be integrated on one single planar substrate with a technology called integrated optics, a basic element of which is the pla-

nar optical waveguide. It consists in a high refractive index guiding core layer of typical dimension 2 μm × 1 μm, sandwiched between two lower-index cladding layers. The optical signal travels in the guiding layer and total internal reflection at the interface between the core and cladding maintains it in the waveguide.

Plastic optical fibers have clear technical advantages over glass fibers: a better flexibility and a large core diameter enabling efficient coupling. If the guiding layer of an optical fiber is doped with an active element, optical gain results upon adequate pumping. Typical low-cost plastic optical fibers of 100 m length have an attenuation of 100 dB·km^{-1} and a bandwidth around 5.1 GHz. More importantly, fluorinated fibers are at hand, with optical transmission extending in the NIR range[57]. This has triggered a large number of projects aiming at synthesizing polymers containing highly luminescent lanthanide complexes, mostly β-diketonates, and displaying large optical gains.

For glass fibers for which direct laser excitation of the Ln^{III} ions is used, the optical gain is calculated as follows. Assuming that the population of the ground state (N_g) of the emitting 4f ion decays rapidly to the first excited state (N_e), the rate equations are those of a two-level system, and further assuming steady state, one gets:

$$N_g = \frac{W_e}{W_e + R} \cdot N \text{ and } N_e = \frac{R}{W_e + R} \cdot N \text{ with}$$

$$R = \frac{\sigma_a P\lambda}{hca} \tag{12}$$

where W_e is the Ln^{III} decay rate, N the Ln^{III} concentration, P the pump power in the waveguide, σ_a the absorption cross section, λ the excitation wavelength, and α the waveguide core cross section. The differential optical gain (OG, in dB·cm^{-1}) is given by:

$$OG = 10 \times {}^{10}\log\frac{I}{I_0} = 10 \times {}^{10}\log(e^{kx}) \text{ with}$$

$$k = \sigma_e \cdot (N_e - N_g) \cdot \alpha \tag{13}$$

in which I_0 is the light intensity at the beginning of the waveguide and I the intensity along the waveguide, k is the optical gain factor, σ_e the emission cross section, and α the fraction of incident light confined in the core of the waveguide. The threshold power, that is the power at which k becomes positive is often much higher for plastic fibers than Er^{III}-doped glasses or alumina amplifiers. This can be traced back to the very small quantum yield of Er^{III} in organic media. But this threshold power can be dramatically reduced if excitation is made in the ligand levels for which the absorption cross section is much larger $\approx 10^3$-fold) Taking the ligand-to-Ln^{III} ion energy

transfer into consideration, calculation of the gain proceeds as follows:

$$\frac{dN_1}{dt} = R_1N_{gl} - W_{1r}N_1 - W_{1nr}N_1N_g \text{ with } R_1 = \frac{\sigma_1 P\lambda}{hca} \quad (14)$$

$$\frac{dN_e}{dt} = -W_eN_e + W_{1nr}N_1N_g \quad (15)$$

in which N_1 and N_e are the population fractions of the excited states of the ligand and Ln$^{\text{III}}$ ion, respectively, while N_{gl} and N_g are the corresponding values for the ground states, W_{1r} and W_{1nr} are the ligand radiative and nonradiative (transfer) decay rates, respectively, while σ_1 is the ligand absorption cross section. The main problem for lanthanide-containing NIR optical fibers is the minimization of nonradiative deactivation of the excited states. Several groups, including industrial laboratories, have devoted large efforts to elaborate strategies addressing this problem[58~60]:

(1) Suppression of vibrational deactivation (including the one induced by water molecules). This problem is usually dealt with by adding long perfluorinated lateral chains on β-diketonates, by deuterating the C-H bridge and by working in deuterated solvents. The longer the perfluorinated chain, the less water molecules penetrate into the inner coordination sphere. They are also expelled by coordination of strong donors such as dmso.

(2) Inhibition of energy migration between luminescent centers and of up-conversion processes. Diffusion of Ln$^{\text{III}}$ chelates in solution induces collisions between molecules, leading to energy transfer via cross-relaxation and excitation migration. Migration of energy by hopping onto a neighboring ion does not quench luminescence by itself, but it enhances the probability of quenching by permitting the energy to finally migrate onto a site where more rapid nonradiative decay takes place. The only way of avoiding this "concentration quenching" is to keep luminescent centers far apart so that the probability of transfer is reduced. This can be done either by having large complexes which possess long fluorinated alkyl chains, or by dispersing them into polymer matrices.

Up-conversion and excited state absorption (ESA) are the main gain-limiting factors in Er$^{\text{III}}$-doped planar optical amplifiers, either glass- or polymer-based. Up-conversion increases 5 ~ 10 fold the pump power required to achieve population inversion. The ESA cross section is strongly material dependent and this phenomenon also increases the pump power needed, so that when both gain-limiting factors are present, pump powers of 10 ~ 100 mW are required, which considerably increases the cost of optical amplifiers. It is hoped that the introduction of sensitizers

such as Yb$^{\text{III}}$, Ag$^{\text{I}}$ or silicon nanocrystals into inorganic optical fibers will help solving this problem. Organic chelates in polymer fibers may also be an alternative[61].

(3) Optimization of the sensitization ability of the ligand and of the emission intensity; η_{sens} for β-diketonates is often between 20% and 30% only but is larger with unsymmetrical ligands compared with symmetrical ones. Adding a second ligand to form a ternary complex, or a dye to transfer energy on the metal ion, improves the sensitization, although it is difficult to go beyond a factor of two, possibly three.

(4) Choice of an adequate host medium and defect-free fabrication of the waveguide. The ideal host should disperse the luminescent centers sufficiently to avoid concentration quenching while simultaneously allowing high enough concentration of these centers and minimizing optical losses. The latter originate from several sources: scattering is a major one and arises from imperfections in the waveguide, such as rough sidewalls or defects in the core material. Another loss mechanism is the mismatch between the device waveguide mode and the incident light source mode. Finally, in a waveguide doped with a chromophoric organic complex, absorption of both the chromophore and the polymer backbone also contributes to the loss. The host material should not modify the complex, or at least not the inner coordination sphere of the luminescent ion, and not provide nonradiative deactivation paths, henceforth the many fluorinated polymers and functionalized zeolites which have been tested.

2.2 Organic light emitting diodes (OLEDs)[14]

A landmark in the development of OLEDs is the finding in 1987 of the bright green emission of aluminum tris(8-hydroxyquinolinate), [Al(8-Q)$_3$], in thin organic layers[62]. This device has a luminance of 1000 cd·m^{-2} with a driving voltage below 10 V and an external quantum efficiency Q_{EL} of 1 photon per 100 electrons injected. For these devices, the external quantum efficiency is defined as:

$$Q_{EL} = \eta_e \times \eta_r \times Q_{PL} \quad (16)$$

where η_e is the fraction of emitted photons coupled out of the device and η_r is the fraction of injected charge carriers that form excitons, while Q_{PL} is the photoluminescence quantum yield.

In 1999, Gillin and Curry demonstrated that tris (8-hydroxyquinolinate) [Er(8-Q)$_3$] displays a broad emission band at room temperature in the range of 380 ~ 750 nm, with a maximum at 600 nm, which is red-shifted by about 80 nm with respect to group III

(e.g., Al$^{\text{III}}$) quinolinates. In addition, a bright 1.54 nm emission is seen upon excitation with an argon laser at 457 nm the intensity of which varies linearly with the excitation power in the range 1 ~ 100 mW[63]. Presently, electroluminescent devices can also be made of a single layer of a π-conjugated polymer, such as poly (phenylene-vinylene), PVV, between two electrodes[14].

Thin film OLEDs consist in multiple organic and/ or metallic layers on an indium-tin oxide (ITO) covered glass deposited by various known methods, plasma deposition, thermal evaporation, Langmuir-Blodgett deposition, or spin-coating from solutions. It is important that the layers are chemically stable and highly transparent to the emitted light. A device with a triple active layer is sketched on Fig. 4: a voltage bias is app lied to the ITO electrodes and electrons and holes are injected in the electron- and hole-transport layers by the cathode and anode, respectively. The voltage bias is not large, but since the layers are very thin (typically a few nm thick), the electric field is in the range of 10^5 ~ 10^7 V·cm^{-1}. Therefore, the injected charges migrate against each other, meet and recombine in the emissive layer. After charge recombination, the hole-transporting layer should also block the migration of excitons from the emitting layer, that is, it should have higher exciton energy than the emissive layer. Among potential materials are poly-(N-vinylcarbazole) (PVK) and N,N-diphenyl-N,N-bis (3-methyl-phenyl)-[1,1'-biphenyl]-4,4'diamine (TPD). Electron-transporting materials widely used are 2-(4-biphenyl)-5-(4-tert-butylphenyl)-1,3,4-oxadiazole or the tris(8-hydroxyquinolinate)aluminum complex.

In OLEDs, 25% of the excitation energy leads to singlet states and 75% to triplet states. As a consequence, it is desirable that the luminescent centers are good triplet quenchers, which is the case of some tran-
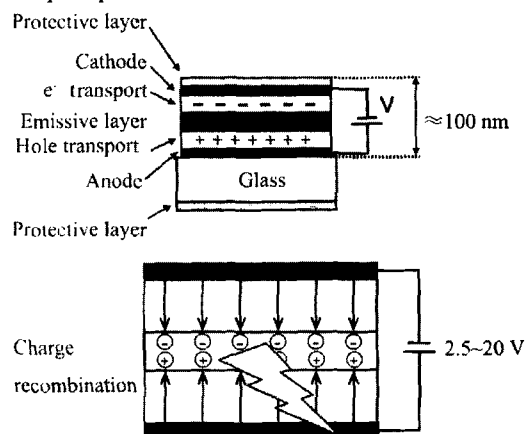
sition metal ions and of lanthanide ions. Amazingly, exploitation of the triplet state energy was ignored until 1998[64] but is now a key goal in the development of these lighting devices. A major challenge in OLEDs is the design of efficient, white-emitting diodes and a recent example demonstrated the feasibility of a lanthanide-based device using up-conversion to produce simultaneous emission of Tm$^{\text{III}}$ at 475 nm, Er$^{\text{III}}$ at 525, 550, and 675 nm, as well as of Eu$^{\text{III}}$ at 590 and 620 nm, upon excitation at 980 nm. The device consists in a sol-gel derived thin film made of Ln$^{\text{III}}$-doped lanthanum fluoride nanoparticles (Ln = Eu, Er, Tm, Yb); the Yb$^{\text{III}}$ ions serving as Er$^{\text{III}}$ sensitizer[65]. Combining Eu$^{\text{III}}$ and Tb$^{\text{III}}$ luminescence of ternary β-diketonate complexes with substrate luminescence from tetraphenyldiamine also generates white light[66]. Another approach is the doping of 2.5% of dendritic Eu$^{\text{III}}$ diketonates such as [Eu(TCPD)$_3$(Phen)] (Fig. 5) into 4,4'-N, N'-dicarbazole biphenyl (CBP). The latter is known for being an excellent host for phosphorescent dopants in view of its high-energy triplet state (≈ 21000 cm^{-1}) and its ambipolar charge-transporting ability. The resulting thin film has been inserted into an electroluminescent device of composition ITO/ NPB/CBP: [Eu(TCPD)$_3$(Phen)]/BCP/Mg:Al, where NPB is (N,N'-bis(1-naphtyl)-N,N'-diphenyl-1,1'-biphenyl-4,4'-diamine) and functions as hole transporter, while BCP is 2,9-dimethyl-4,7-diphenyl,1,10-phenanthroline and serves as a hole blocker. External quantum yields around 1% are achieved with a current density of 50 mA·cm^{-2} at a driving voltage of 16 V[67]. The suitability of coordination complexes of d- and f-transition elements as triplet emitters in OLEDs has recently been discussed and more information can be found in this comprehensive review article[9].
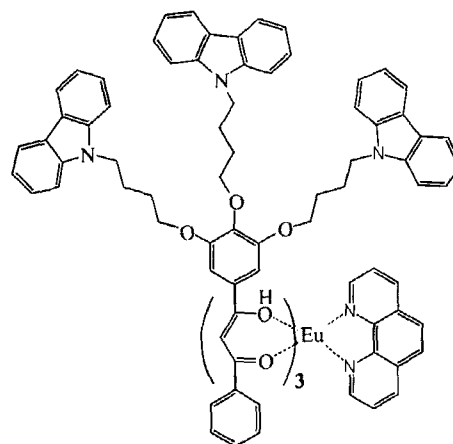

Fig. 4 Scheme of an organic light emitting diode (OLED)

Fig. 5 [Eu(TCPD)$_3$(Phen)] dendrimeric complex used for electroluminescent white-light emission[67]

3 Lanthanide Luminescence for Biomedical Imaging and Sensing

Interaction between lanthanides and biological tissues or organs has been studied for almost one hundred years. For instance, the inhibitory effect of lanthanide ions on the beating of perfused frog hearts has been described in 1910 already[68]. In the 1960's through the 1980's, attention was devoted to the fact that Ln^{III} ions easily replace Ca^{II} ions owing to their similar ionic radii, water exchange rates and coordination numbers[69]. Lanthanide ions were used either as luminescent structural probes for large biological molecules[70] or for the study of cellular calcium fluxes. In fact, simple lanthanide compounds mainly interact with cell membranes, which results in perturbations in the cellular transport of metal ions. This phenomenon and the effects of lanthanides on the cellular metabolism have been investigated in details for cardiac, nervous, and adrenal tissues, as well as for smooth muscles, skeletal muscles, platelets, mast cells, erythrocytes, leukocytes, and amphibian bladder and skin, among others. In parallel, extensive toxicological studies have been undertaken[68].

Luminescence and radioactive analyses of biological materials are among the most sensitive analytical techniques known. At the end of the 1980's, a research team in Turku (Finland) proposed to take advantage of the long excited states of the lanthanide ions to develop time-resolved luminescence immunoassays (TRL-IA). Because the autofluorescence of the samples can be avoided in this way, and because the overall time needed to perform one measurement is very short (1 ~ 2 ms) allowing the accumulation of thousands of measurements within minutes, TRL-IA rapidly became extremely popular. Indeed, they compete efficiently with radio-tracer methods while not having their drawback, that is the cumbersome elimination of radioactive wastes[71]. This fact and the body of works at hand on the interaction between lanthanides and biological materials led to the rapid development of analytical sensors[72] and cell imaging stains[73].

Until recently, molecular probes for luminescence sensing or imaging applications were mostly based on heterocyclic aromatic dyes, e. g., rhodamine. These sensors, of which hundreds are commercially available, rely on fluorescence and their main advantages lie in large molar absorption coefficients and quantum yields, as well as in their being relatively easy to conjugate with biomolecules[74]. On the other hand, these luminescent stains are often prone to interferences from both the autofluorescence of the analyzed sample and scattered light. In addition, they have short-lived excited states with lifetime in the nanosecond range, and display broad emission bands with small Stokes' shifts, in addition to being sensitive to photobleaching. To remedy to some of these drawbacks, authors have turned either to quantum dots or to metal complexes[75]. Semi-conductor quantum dots[76] (e.g., CdSe, InN) have very large absorption coefficients ($> 10^6$ $M^{-1} \cdot cm^{-1}$) and their emission bandwidth depends on the particle size, that is it can be tuned. Metal coordination compounds, particularly lanthanide complexes, have three advantages: easily recognizable, line-like emission spectra, long lifetimes, and relative insensitivity to photo-bleaching. As mentioned above, synthetic chemists have learned how to design adequate molecular assemblies for hosting these ions and also for coupling the resulting complexes to biomolecules[16, 77]. In addition to luminescent immunoassays, two lines of research are particularly active presently, the search for near-infrared sensors and the design of luminescent stains for specific *in cellulo* sensing and imaging.

3.1 Going into near-infrared

Although bioanalyses and bio-imaging have been the driving force of many investigations during the last decade, very few systems have made it up to real applications at least as far as NIR luminescence is concerned[18]. There are two major applications for which NIR probes are being searched for: luminescent immunoassays and diagnosis of tumors (cell imaging). Since Yb^{III} is the NIR-emitting ion having usually the best quantum yield, most of the biomedical applications published to date use this ion. The incentive for designing NIR-emitting probes rather than visible-emitting ones is the fact that the former may be more easily excited by visible light, instead of UV-light which may damage biological molecules, in addition to biological tissues being optically transparent in the range 0.7 ~ 1 μm[78].

The possibility of using Yb^{III} luminescence for the diagnosis of tumors has been described in 1989 already for porphyrinate complexes. Porphyrins have the ability to accumulate in cancer cells or, more generally, in fast growing tissues, so that they are presently being explored in a number of medical applications ranging from cancer therapy (the best known application), to cardiology, ophthalmology, or dermatology[79, 80]. Haematoporphyrins accumulate more efficiently in malignant tumor than porphyrins and are therefore privileged targets for photodynamic treat-

ment of cancer. On the other hand, they have two disadvantages: (1) a high phototoxicity, which requires protection of patients from the action of light on the skin, and (2) a low contrast of tumors caused by the masking effect of the background fluorescence. These disadvantages can be overcome, at least in principle, by the use of the 1 μm emission line of Yb^{III}, since the luminescence of the latter is distinct from the emission of the ligand. Haematoporphyrins initially provided for the diagnosis of malignant tumors are sketched on Fig. 6[81,82]. The poorly soluble Yb^{III} complexes were introduced into phosphatidylcholine liposomes and metal ion luminescence was monitored from sarcoma-implanted mice. Both the central and peripheral regions of the tumors were imaged, as well as the surrounding healthy skin, which allowed the calculation of a contrast ratio γ_s from the total emission areas S (emission from tumor) and S_0 (emission from healthy skin):

$$\gamma_s = \frac{S - S_0}{S} \qquad (17)$$

The complexes $[Yb(1a)]^+$ and $[Yb(1c)]^{3-}$ yield a contrast value $\gamma_s = 10 \pm 2$, while the two other complexes are more efficient, with γ_s values equal to 19 ± 4, and 45 ± 9 for $[Yb(1b)]^-$ and $[Yb(1d)]^{3-}$, respectively. In addition to the lower phototoxicity of the lanthanidoporphyrinates these contrast data compare most favorably with those obtained with porphyrins alone (1.1 - 1.2). The affinity of porphyrin for cancer cells increases when metalloporphyrin-albumin conjugates are used and therefore, $[Yb(H_3 1c)]$ $(im)_2]$ (see Fig. 6, im is imidazole) has been conjuga-

ted, in two steps, with bovine serum albumin (BSA) which contains free amino groups from lysine residues located at its surface. The number of porphyrin molecules per protein was in the range 5.4 ~ 6.6. With respect to $[Yb(H_3 1c)(im)_2]$, which has a quantum yield of 0.6% in water at pH 9.2, the fluorescence of the BSA conjugate is three-fold larger[83].

One of the few present practical applications of NIR-emitting probes is the elegant technology proposed by a group from Leiden University who developed a luminescent reporter for the sensitive detection of antigens in tissue sections or on cell membranes. The method does not rely on NIR luminescence but, rather, on NIR excitation followed by up-conversion. It consists in microcrystals (0.2 ~ 0.4 μm) made of yttrium oxysulfide, fluoride, silicate, or gallate doped with two different lanthanides and exhibiting strong emission in the visible (blue, green, and red). The microparticles are surface-labeled with avidin or antibodies and can bind specifically to antigens on intact cells or in tissue sections. The phosphor microparticles exhibit visible luminescence by up-converting infrared to visible light. The method is termed up-converting phosphor technology (UPT) and has been tested on the prostate-specific antigen in tissue sections and the CD4 membrane antigen on human lymphocytes[84]. The same technology has now been applied to a competitive homogeneous immunoassay for 17-estradiol in serum, using a small-molecular dye as an acceptor. Sensitized acceptor emission was measured at 600 nm under continuous laser diode excitation at 980 nm with lower limits of detection < 1 nmol $\cdot L^{-1}$. This novel principle has unique advantages compared to present homogeneous luminescence-based methods and leads to attractive assay systems for clinical diagnostics and high-throughput screening approaches[85].

Several strategies have been proposed for encapsulating NIR-emitting Ln^{III} ions which have been recently reviewed by the authors[46]. In our laboratory, the approach makes use of podands fitted with 8-hydroxyquinoline pendant arms, for instance the tetrapodal ligand H_8 2 (Fig. 7). The spacer bears an amide coupling function and its length is chosen to achieve a tight coordination around the Ln^{III} ion, saturating its first coordination sphere. The ligand interacts fairly strongly with trivalent lanthanide ions in water yielding 1:1 podates with pLn values in the range of 15 ~ 16 (The pLn values are defined as $-\log_{10} [Ln]_{free}$ at pH 7.4 and for $[Ln]_{tot} = 10^{-6}$ M and $[L]_{tot} = 10^{-5}$ M[86]). Several species are in equilibrium but fortunately, the 1:1 $[Ln(H_2 2a)]^{3-}$ species is largely dominant in the pH range 6 ~ 8. The Nd^{III} and

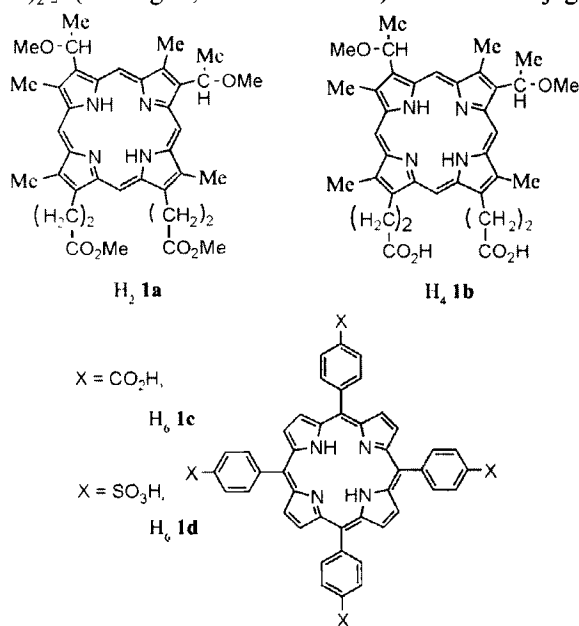Yb^{III} podates are quite luminescent and hydration numbers calculated from lifetimes in water and deuterated water are very small, indicating a well protective cavity induced by the coordinated podand. Improvement in the photophysical properties is achieved by methylating the secondary amine groups in podand H$_8$2b, which again points to the importance of high-energy vibrators in the second coordination sphere. The quantum yield obtained for Yb^{III} is so far one of the largest reported for a molecular compound in aqueous solution, 0.37%. It is 4- and 15-fold larger than the quantum yields found for complexes with fluorexon[87] and tropolonate[88], for instance. The overall luminescence efficiency of the [Yb(H$_2$2b)]$^{3-}$ podate, $\varepsilon \cdot Q_{Ln}^L$, reaches 70 M$^{-1} \cdot$cm^{-1} for an excitation at 344 nm and excitation up to 580 nm is possible. The podate [Yb(H$_2$2b)]$^{3-}$ has been successfully introduced into a glass matrix using a two-step sol-gel method and thin films of this material display even better photophysical properties than the aqueous solutions, with an average quantum yield of 0.45%, which is encouraging with respect to potential applications[89].

Following a slightly different strategy, we have designed a tripodal ligand, H$_6$3 (Fig. 7), consisting in a triamine anchor bearing three 8-hydroxyquinoline units which are tailored to behave as tridentate receptors. As for the tetrapodal ligands, highly stable and

water soluble 1:1 complexes are formed and the three Nd^{III}, Er^{III}, and Yb^{III} chelates display sizeable metal-centered NIR luminescence in aqueous solutions at pH 7.4, but the quantum yields are somewhat smaller than for the podates with ligand H$_2$2b. On the other hand, cytotoxicity studies on several cell lines have shown the Yb^{III} chelate to be non-toxic, opening the way for applications in cell sensing and/or imaging[90]. Further improvement of the photophysical properties will have to go through fluorination of the ligands, or to the use of iminodiphosphinate "shell" ligands[91].

The NIR-emitting Ln^{III} ions have the tendency to display relatively short excited state lifetimes (in the microsecond range). Although time-resolved luminescence is still feasible, longer lifetimes would lead to simpler instrumentation. Therefore we have also attempted to lengthen the apparent lifetime of the emitting state by feeding it with a long-lived species such as Cr^{III}. The corresponding bimetallic edifice is sketched on Fig. 8 along with the formula of the corresponding pentadentate ligand 4. Under stoichiometric conditions, the ligand self-assembles with equivalent quantities of Cr^{III} and Yb^{III} ions to yield a stable triple-stranded helicate in which the two metal ions are separated by 0.93 nm. Excitation of the Cr^{III} ion through the ligand states results in a directional energy transfer populating the Yb^{III} (^{2}F$_{5/2}$) level which emits
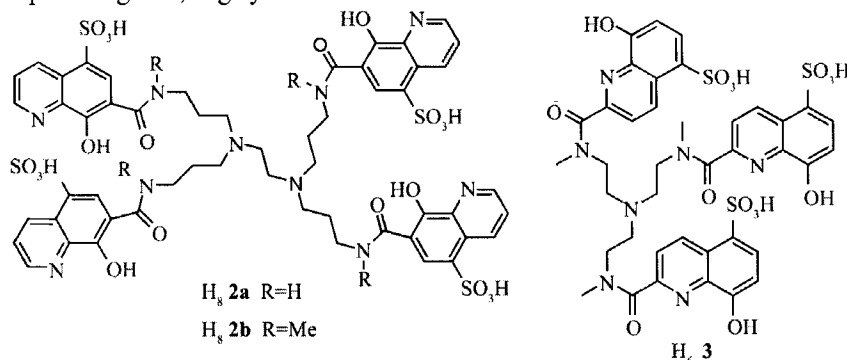

H$_8$ 2a R=H
H$_8$ 2b R=Me

H$_6$ 3

Fig. 7 Tetra- and tri-podal ligands fitted with 8-hydroxyquinoline sensitizing groups
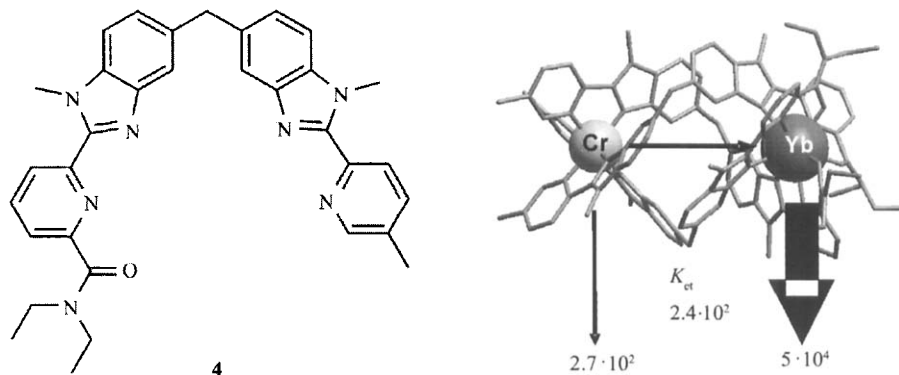

4

K_{et}
2.4·10^2

2.7·10^2

5·10^4

Fig. 8 Ditopic pentadentate ligand for self assembly of 3d-4f edifices (left) and structure and photophysical parameters of Cr^{III}-Yb^{III} complex (right)

its characteristic light with an apparent lifetime equal to that of the Cr(^{2}E) level (2 ms at 10 K). The yield of the directional transfer amounts to 45% for Yb^{III} while it is much larger for Nd^{III}, 87% [92, 93].

3.2 In cellulo sensing and imaging [18, 73]

In view of the large success sustained by time-resolved luminescent immunoassays [16, 94] and DNA labelling [95], a logical expansion is to try to use similar lanthanide-tagged labels for *in cellulo* analyses and cell imaging. While *in vitro* experiments are easily feasible, *in vivo* analyses may be more difficult to implement, unless near-IR emitting probes are used (see above section) or convenient two-photon excitation of Eu^{III} and Tb^{III} probes [96, 97] can be achieved. These aspects start to be investigated and published results to date are encouraging.

To our knowledge, the first experiments of staining cells with lanthanide complexes date back to 1969 when Scaff W L et al. treated bacterial smears (*E. Coli* cell walls) with aqueous ethanolic solutions of europium thenoyltrifluoroacetonate (tta) 1 mM and observed the red emission of Eu^{III} under mercury lamp excitation at 365 nm [98]. In another earlier work, clinically relevant concentrations of adriamycin were found to quench Tb^{III} luminescence from GH3/B6 pituitary tumor cells incubated with 50 μM terbium chloride. Comparison with the quenching by cis-platin suggested that, in the plasma membrane of tumorigenic cells, adriamycin and cisplatin receptor sites are associated with the same calcium-binding protein [99]. The usefulness of lanthanide probes for eliminating the autofluorescence background by time-resolved detection was demonstrated with a Tb^{III} conjugate, formed from a diethylenetriaminepentaacetate (dtpa) chelate sequentially reacted with 4-aminosalicylate and dioleoylphosphatidylethanolamine. This probe has been used successfully as a membrane-staining agent for morphological studies of 3T3 cultured cells [100]. Thermal imaging is also feasible. For instance, metabolic heat signals generated by ligand-receptor interactions in Chinese hamster ovary (CHO) cells have been evidenced with a europium thenoyltrifluoroacetonate sensor, the phosphorescence of which decreases with increasing temperature. Heat wave could be recorded and followed at about 1 s intervals [101].

The group of Bornhop D J has come up with an extensive work based on ligand H$_3$5 (Fig. 9), the Tb^{III} complex of which has superior properties for use as an abnormal tissue marker. The chelate has low toxicity, attractive luminescent properties, rapid pharmokinetics , and relatively high water solubility . It can be
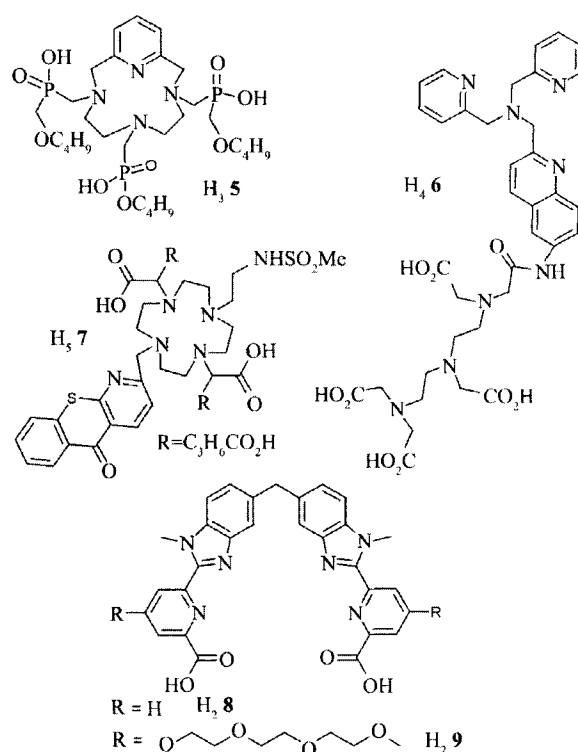
Fig. 9   Ligands used for cell imaging

quantified at the picomolar level in tissues and shows significant difference in affinity for adenocarcinoma cells HT-29 versus normal epithelial cells (IEC-6), or for the imaging of C6 glioblastoma (brain cancer) cells over-expressed with respect to their peripheral benzodiazepine receptors [102~104].

In cellulo sensing is crucial to many biological studies, including unraveling the mechanism of cell apoptosis. Nagano T and collaborators have derivatized diethylenetriamine-pentaaceticacid (dtpa) bisamide with a zinc binding unit, N,N,N',N'-tetrakis(2-pyridylmethyl)ethylenediamine (TPEN) and have shown the Tb^{III} luminescence of the resulting chelate showing a remarkable increase upon addition of Zn^{II} in HEPES buffer [105]. The Eu^{III} complex with dtpa monoamide monosubstituted with 2-N, N-bis (2-pyridylmethyl)-aminomethylquinolin (H$_4$6, see Fig. 9) also display tunable luminescence with high selectivity for Zn^{II} and its usefulness for monitoring zinc concentration changes in human cervical adenocarcinoma (HeLa) cells has been demonstrated [106]. A leader in the field is Durham-based David Parker's group who has proposed an extensive series of luminescent lanthanide chelates with derivatized cyclens, both as responsive sensors for pH, pO$_2$ and selective anions analysis [72, 107] and as stains for cell imaging [73]. Several of the latter in cellulo probes have quantum yields in the range 5% ~ 10% in water and can be excited at the beginning of

the visible range (> 340 nm). An example is the bi-functional anionic complex $[Eu(7)]^{2-}$ (Fig. 9) in which the azathiaxanthone acts as chromophoric antenna while the sulfonamide substituent binds the metal in a pH-dependent manner, being coordinated at high pH and unbound at low pH. In the latter case, the free coordination position is occupied by a water molecule which partly quenches the Eu^{III} luminescence. Mouse skin fibroblasts NIH-3T3 cells uptake the complex which localizes in the nucleolus, allowing its staining[108].

Recently, an elegant method has been proposed for the detection of singlet oxygen based on a europium complex with a terpyridine fitted with four carboxylic acid groups and a methyl-9-anthryl chromophoric antenna. Reaction with $^1\Delta$ O_2 results in the rapid formation ($k = 1 \times 10^{10}$ $M^{-1} \cdot s^{-1}$) of an endoperoxide accompanied by a large increase in the quantum yield. The water-soluble probe is easily transferable into HeLa cells by incubation with tetra-methylpyridinioporphyrine tetra (p-toluenesulfonate) and time-dependent generation of singlet oxygen into the cells can be monitored in time-resolved mode[109].

In our group, we have been designing ditopic hexadentate ligands which self-assemble with lanthanide ions to yield homo- or hetero-bimetallic helicates

with 2:3 Ln:L stoichiometry[55, 56], with the ultimate goal of synthesizing bi-functional luminescent probes[110]. For instance, unsubstituted ligand H_2**8** (Fig. 9) leads to highly stable edifices in water ($log\beta_{23}$ = 26 for Eu) with a quantum yield of 25% (The reported value of 1.3% is in gross error and has been re-determined recently in the authors' laboratories by two independent experimental techniques[111]). To enhance solubility of the neutral helicates and, possibly to ease their uptake in biological cells, a polyoxyethylene arm has been grafted on the 4 position of the pyridine moieties H_2**9**. Similarly to H_2**8**, this new ligand yields stable helicates ($log\beta_{23}$ in the range of 26 ~ 30) and good sensitization of Eu^{III} luminescence is reflected in a quantum yield amounting to 18% at physiological pH and a lifetime of the $^5D_0$ level of 2.4 ms. The helicate permeates readily into HeLa cells and stains their cytoplasm in a concentration-dependent manner (Fig. 10). Excitation up to 405 nm (a wavelength routinely employed in confocal microscopy) is feasible and the complex displays no cytotoxicity up to a concentration of 500 μM[112]. The ligand also sensitizes other Ln^{III} ions, which opens the way for the development of a wide series of cell markers.
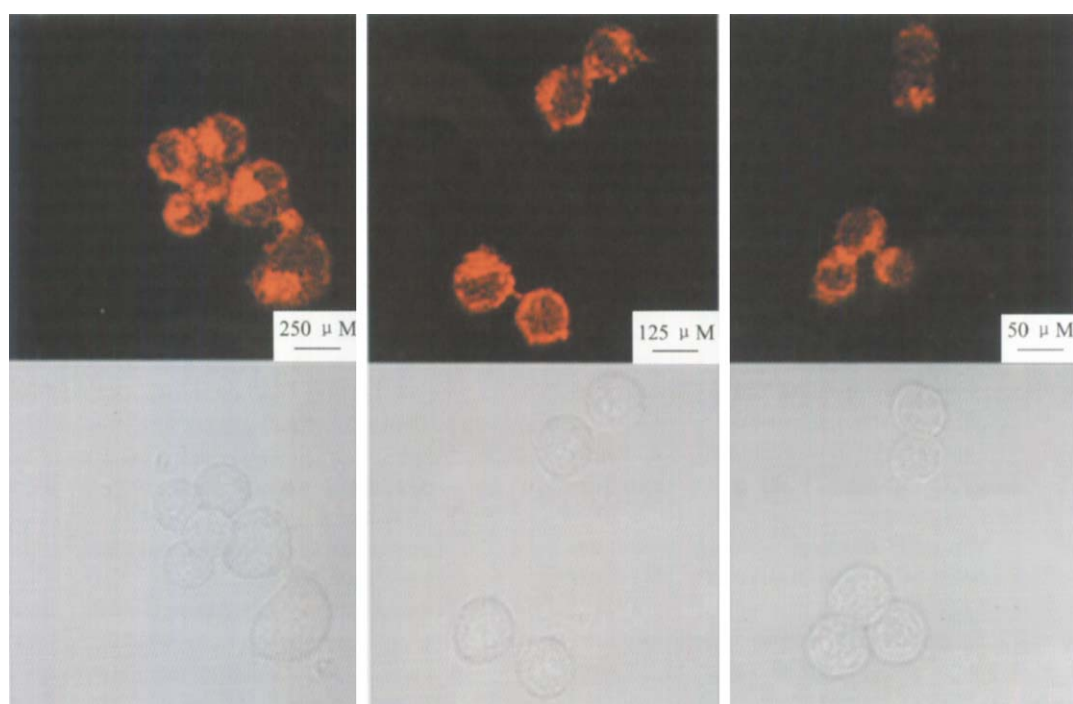

Fig. 10   Staining of Hela cells with$[Eu_2(9)_3]$. The cells were incubated in the presence of different concentrations of the complex in RPMl-1640 for 6 h at 37 °C. The images were taken using a Zeiss LSM 500 META confocal microscope (objective: Plan-Apochromat, 63/1.30 oil ; Eu^{III} luminescence excited at 405 nm and detected after filtration with an LP 505 filter). Scale bar: 17 μm.

4 Conclusion

In this short overview of selected current trends in lanthanide luminescence, we have tried to exemplify the new possibilities offered by lanthanides in fields as far apart as materials science and medical diagnosis. There are numerous themes which have not been evoked here, luminescent thermotropic liquid crystals[113, 114, 15], ionogels[115], nanomaterials[116], nanocapsules[117], long-persistence phosphors[118], or nonlinear optical properties[119], for instance. As far as biological analyses and medical diagnosis are concerned, designing systems allowing multiphoton excitation (particularly two-photon absorption) and preventing de-activation processes are the main challenges presently. The wide choice of luminescence properties displayed by lanthanide ions, as well as the well-mastered introduction of these ions into a wealth of different molecular and extended structures such as coordination polymers[120,121] and microporous materials[122], is a fantastic playground for scientists and engineers. The lanthanides will be key elements in helping scientists to meet all the future technological challenges, including solving the energy problem. They will also boost our capability to monitor biological processes essential to life and help physicians curing major diseases such as cancer. We hope that this review will encourage young investigators to join the growing community who is already exploiting the fascinating properties of lanthanides for offering a better living to the inhabitants of planet earth.

References:

[1] Niinistö L. Discovery and Separation of Rare Earths, in Rare earths [M]. Eds. Puche R Saez and Caro P, Editorial Complutense, Madrid, 1998. 25.

[2] Chen M. Introduction, in Rare Earth Elements and Their Applications [M]. Eds. Yu Z and Chen M. Beijing: Metallurgical Industry Press, 1995.

[3] Gadolin J. Underfökning af en fvart tung stenart ifrän ytterby stenbrott i roflagen [J]. Kungl. Sv. Vetenskapsak. Handl., 1794, 55: 137.

[4] Gadolin J. Von einer schwarzen, schweren steinart aus ytterby steinbruch in roslagen in schweden [J]. Crells chem. Ann., 1796. 313.

[5] Cotton S. Lanthanide and Actinide Chemistry, Inorganic Chemistry, a Wiley Textbook Series [M]. Chichester: John Wiley & Sons Ltd., 2006.

[6] Bünzli J-C G. Benefiting from the unique properties of lanthanide Ions [J]. Acc. Chem. Res., 2006, 39: 53.

[7] Ozawa L, Itoh M. Cathode ray tube phosphors [J]. Chem. Rev., 2003, 103: 3835.

[8] Shionoya S, Yen W M. Phosphor Handbook [M]. Boca Raton, FL 33431, USA: CRC Press Inc., 1999.

[9] Evans R C, Douglas P, Winscom C J. Coordination complexes exhibiting room-temperature phosphorescence: Evaluation of their suitability as triplet emitters in organic light emitting diodes [J]. Coord. Chem. Rev., 2006, 250: 2093.

[10] Bünzli J-C G, Choppin G R. Lanthanide Probes in Life, Chemical and Earth Sciences: Theory and Practice [M]. Amsterdam: Elsevier Science Publ. B.V., 1989.

[11] Hemmilä I, Ståhlberg T, Mottram P. Bioanalytical Applications of Labelling Technologies [M]. Wallac Oy, Turku, 1995.

[12] Bünzli J-C G. Rare Earth Luminescent Centers in Organic and Biochemical compounds, in Spectroscopic Properties of Rare Earths in Optical Materials, Springer Series in Materials Science [M]. Eds. Liu G K and Jacquier B, Berlin: Springer Verlag, 2005. 462.

[13] Bünzli J C G, Piguet C. Taking advantage of luminescent lanthanide ions [J]. Chem. Soc. Rev., 2005, 34: 1048.

[14] Kido J, Okamoto Y. Organolanthanide metal complexes for electroluminescent materials [J]. Chem. Rev., 2002, 102: 2357.

[15] Terazzi E, Suárez S, Torelli S, Nozary H, Imbert D, Mamula O, Rivera J P, Guillet E, Benech J M, Bernardinelli G, Scopelliti R, Donnio B, Guillon D, Bünzli J C G, Piguet C. Introducing bulky functional lanthanide cores into thermotropic metallomesogens: a bottom-to-top approach[J]. Adv. Func. Mater., 2006, 16: 157.

[16] Matsumoto K, Yuan J G. Lanthanide Chelates as Fluorescent Labels for Diagnostics and Biotechnology, in Metal Ions in Biological Systems [M]. Eds. Sigel A and Sigel H, New York: Marcel Dekker Inc., 2003. 40.

[17] Faulkner S, Matthews J L. Fluorescent Complexes for Biomedical Applications, in Comprehensive Coordination Chemistry II [M]. Ed. Ward M D, Amsterdam: Elsevier Pergamon, 2004, 9. 913.

[18] Faulkner S, Pope S J A, Burton-Pye B P. Lanthanide complexes for luminescence imaging applications [J]. Appl. Spectrosc. Rev., 2005, 40: 1.

[19] Shionoya S, Yen W M. Principal Phosphor Materials and Their Optical Properties, in Phosphor Handbook [M]. Eds. Shionoya S and Yen W M, Boca Raton, FL 33431, USA: CRC Press Inc., 1999. 177.

[20] Blasse G. The Influence of charge-transfer and rydberg states on the luminescence properties of lanthanides and actinides[J]. Struct. Bond., 1976, 26: 45.

[21] Dorenbos P. The 4f to 4f5d transitions of the trivalent lanthanides in halogenides and chalcogenides[J]. J. Lumin., 2000, 91: 91.

[22] Carnall W T. The Absorption and Fluorescence Spectra of Rare Earth Ions in Solution, in Handbook on the Physics and Chemistry of Rare Earths [M]. Eds. Gschneidner K A Jr and Eyring L, Amsterdam: North Holland Publ. Co., 1979, 3: 172.

[23] de Sá G F, Malta O L, Donega C D, Simas A M, Longo R L, Santa-Cruz P A, da Silva E F. Spectroscopic properties and design of highly luminescent lanthanide coordination complexes[J]. Coord. Chem. Rev., 2000, 196:165.

[24] Gonçalves e Silva F R, Malta O L, Reinhard C, Güdel H U, Piguet C, Moser J E, Bünzli J-C G. Visible and near-infrared luminescence of lanthanide-containing dimetallic triple-stranded helicates: energy transfer mechanisms in the Sm(III) and Yb(III) molecular edifices[J]. *J. Phys. Chem. A*, 2002, **106**: 1670.

[25] Vila Nova S P, Pereira G A L, Albuquerque R Q, Mathis G, Bazin H, Autiero H, de Sa G F, Alves S. Study of the luminescence of Eu(III), Tb(III) and Gd(III) cryptates containing Py (CO2Et)(2) as ligands[J]. *J. Lumin.*, 2004, **109**: 173.

[26] Baek N S, Kim Y H, Roh S G, Kwak B K, Kim H K. The first Inert and photostable encapsulated lanthanide (III) complexes based on dendritic 9,10-diphenylanthracene ligands: synthesis, strong near-infrared emission enhancement, and photophysical studies[J]. *Adv. Func. Mater.*, 2006, **16**: 1873.

[27] Cantuel M, Gumy F, Bünzli J-C G, Piguet C. Encapsulation of labile trivalent lanthanides into a homobimetallic chromium(III)-containing triple-stranded helicate. Synthesis, characterization, and divergent intramolecular energy transfers[J]. *Dalton Trans.*, 2006, 2647.

[28] Kennedy F, Shavaleev N M, Koullourou T, Bell Z R, Jeffery J C, Faulkner S, Ward M D. Sensitised near-infrared luminescence from lanthanide(III) centres using Re(I) and Pt(II) diimine complexes as energy donors in d-f dinuclear complexes based on 2,3-bis (2-pyridyl) pyrazine[J]. *Dalton Trans.*, 2007, 1492.

[29] Guo D, Duan C, Lu F, Hasegawa Y, Meng Q, Yanagida S. Lanthanide heterometallic molecular squares Ru2-Ln2 exhibiting sensitized near-infrared emission [J]. *Chem. Commun.*, 2004, 1486.

[30] Le Quang A Q, Zyss J, Ledoux I, Truong V G, Jurdyc A M, Jacquier B, Le D H, Gibaud A. An hybrid organic-inorganic approach to erbium-functionalized nanodots for emission in the telecom window[J]. *Chem. Phys.*, 2005, **318**: 33.

[31] Zolin V F, Puntus L N, Tsaryuk V I, Kudryashova V A, Legendziewicz J, Gawryszewska P, Szostak R. Spectroscopy of europium and terbium pyridine-carboxylates[J]. *J. Alloys Comp.*, 2004, **380**: 279.

[32] Kim Y H, Baek N S, Kim H K. Sensitized emission of luminescent lanthanide complexes based on 4-naphthalen-1-yl-benzoic acid derivatives by a charge-transfer process[J]. *Chem. Phys. Chem.*, 2006, **7**: 213.

[33] Puntus L N, Chauvin A S, Varbanov S, Bünzli J-C G. Lanthanide complexes with a calix[8] arene bearing phosphinoyl pendant arms[J]. *Eur. J. Inorg. Chem.*, 2007, Published on the web, April 17, 2007 DOI 10. 1002/ejic.200601180

[34] Lazarides T, Alamiry M A H, Adams H, Pope S J A, Faulkner S, Ward M D. Anthracene as a sensitiser for near-infrared luminescence in complexes of Nd(III), Er (III) and Yb(III): an unexpected sensitisation mechanism based on electron transfer [J]. *Dalton Trans.*, 2007, 1484.

[35] Petoud S, Bünzli J C G, Glanzman T, Piguet C, Xiang Q, Thummel R P. Influence of charge-transfer states on the Eu(III) luminescence in mononuclear triple helical

[36] Gonçalves e Silva F R, Longo R L, Malta O L, Piguet C, Bünzli J C G. Theoretical modelling of the low quantum yield observed in an Eu(III) triple helical complex with a tridentate aromatic ligand [J]. *Phys. Chem. Chem. Phys.*, 2000, **2**: 5400.

[37] Chauvin A S, Gumy F, Imbert D, Bünzli J C G. Europium and terbium tris(dipicolinates) as secondary standards for quantum yield determination [J]. *Spectrosc. Lett.*, 2004, **37**: 517; erratum, 2006, 40: 193.

[38] de Mello J C, Wittmann H F, Friend R H. An improved experimental determination of external photoluminescence quantum efficiency[J]. *Adv. Mat.*, 1997, **9**: 230.

[39] Görller-Walrand C, Binnemans K. Spectral Intensities of f-f transitions, in Handbook on the Physics and Chemistry of Rare Earths [M]. Eds. Gschneidner K A Jr and Eyring L, Amsterdam: Elsevier Science B. V., 1998, **25**: Ch.167.

[40] Judd B R. Optical Absorption Intensities of Rare Earth Ions[J]. *Phys. Rev.*, 1962, **127**: 750.

[41] Ofelt G S. Intensities of crystal spectra of rare earth Ions[J]. *J. Chem. Phys.*, 1962, **37**: 511.

[42] Nielson C W, Koster G F. Spectroscopic Coefficients for pn, dn, and fn Configurations [M]. Cambridge (Massachussetts): MIT Press, 1963.

[43] Carnall W T, Fields P R, Wybourne B G. Spectral Intensities of the Trivalent Lanthanides and Actinides in Solution.I. Pr(III), Nd(III), Er(III), Tm(III), Yb(III)[J]. *J. Chem. Phys.*, 1965, **42**: 3797.

[44] Werts M H V, Jukes R T F, Verhoeven J W. The e-mission spectrum and the radiative lifetime of Eu³⁺ in luminescent lanthanide complexes [J]. *Phys. Chem. Chem. Phys.*, 2002, **4**: 1542.

[45] Martel l A E, Hancock R D, Motekaitis R J. Factors affecting stabilities of chelate, macrocyclic and macrobicyclic complexes in solution[J]. *Coord. Chem. Rev.*, 1994, **133**: 39.

[46] Comby S, Bünzli J C G. Lanthanide Near-Infrared Luminescence in Molecular Probes and Devices, in Handbook on the Physics and Chemistry of Rare Earths [M]. Eds. Jr. Gschneidner K A, Bünzli J C G, Pecharsky V K, Amsterdam: Elsevier Science B.V., 2007, **37**: 235, in press.

[47] Quochi F, Orru R, Cordella F, Mura A, Bongiovanni G, Artizzu F, Deplano P, Mercuri M L, Pilia L, Serpe A. Near infrared light emission quenching in organolanthanide complexes [J]. *J. Appl. Phys.*, 2006, **99**: 053520 - 1 - 053520 - 4.

[48] Yang Y S, An B, Gong M L, Shi H H, Lei H Y, Meng J X. Progress on study of luminescence of rare earth organic chelates[J]. *J. Rare Earths*, 2002, **20**: 161.

[49] Choppin G R. A half-century of lanthanide aminopolycarboxylates[J]. *J. Alloys Comp.*, 1993, **192**: 256.

[50] Binnemans K. Rare earth b-diketonate Complexes: Functionalities and Applications, in Handbook on the Physics and Chemistry of Rare Earths [M]. Eds. Jr Gschneidner K A, Bünzli J C G, Pecharsky V K, Am-

sterdam: Elsevier Science B.V., 2005, **35**: 225.

[51] Vigato P A, Tamburini S. The challenge of cyclic and acyclic schiff bases and related derivatives [J]. *Coord. Chem. Rev.*, 2004, **248**: 1717.

[52] Sastri V S, Bünzli J C G, Rao V R, Rayudu G V S, Perumareddi J R. Modern Aspects of Rare Earths and Complexes [M]. Amsterdam: Elsevier Science B. V., 2003.

[53] Ng D K P. Half-sandwich tetrapyrrole complexes of rare earths and actinides, in Handbook on the Physics and Chemistry of Rare Earths [M]. Eds. Jr Gschneidner K A, Eyring E M, Lander G H, Amsterdam: Elsevier Science B V, 2001, **32**: 210.

[54] Asfari Z, Böhmer V, Harrowfield J M, Vicens J. Calixarenes 2001 [M]. Dordrecht: Kluwer Academic Publishers, 2001.

[55] Bünzli J C G, Piguet C. Lanthanide-containing molecular and supramolecular polymetallic functional assemblies [J]. *Chem. Rev.*, 2002, **102**: 1897.

[56] Piguet C, Bünzli J C G. Mono- and polymetallic lanthanide-containing functional assemblies: a field between tradition and novelty [J]. *Chem. Soc. Rev.*, 1999, **28**: 347.

[57] Kuriki K, Koike Y, Okamoto Y. Plastic optical fiber lasers and amplifiers containing lanthanide complexes [J]. *Chem. Rev.*, 2002, **102**: 2347.

[58] Yanagida S, Hasegawa Y, Murakoshi K, Wada Y, Nakashima N, Yamanaka T. Strategies for enhancing photoluminescence of Nd^{3+} in liquid media [J]. *Coord. Chem. Rev.*, 1998, **171**: 461.

[59] Hasegawa Y, Wada Y, Yanagida S. Strategies for the design of luminescent lanthanide(III) complexes and their photonic applications [J]. *J. Photochem. Photobiol. C: Photochem. Rev.*, 2004, **5**: 183.

[60] Slooff L H, van Blaaderen A, Polman A, Hebbink G A, Klink S I, Van Veggel F C J M, Reinhoudt D N, Hofstraat J W. Rare-earth doped polymers for planar optical amplifiers [J]. *J. Appl. Phys.*, 2002, **91**: 3955.

[61] Polman A, Van Veggel F C J M. Broadband sensitizers for erbium-doped planar optical amplifiers: review [J]. *J. Opt. Soc. Am. B. Opt. Physics*, 2004, **21**: 871.

[62] Tang C W, Van Slyke S A. Organic electroluminescent diodes [J]. *Appl. Phys. Lett.*, 1987, **51**: 913.

[63] Gillin W P, Curry R J. Erbium (III) tris (8-hydroxyquinoline) (ErQ): A potential material for silicon compatible 1.5 mu m emitters [J]. *Appl. Phys. Lett.*, 1999, **74**: 798.

[64] Baldo M A, O'Brien D F, You Y, Shoustikov A, Sibley S, Thompson M E, Forrest S R. Highly efficient phosphorescent emission from organic electroluminescent devices [J]. *Nature*, 1998, **395**:151.

[65] Sivakumar S, vanVeggel F C J M, Raudsepp M. Bright white light through Up-conversion of a single NIR source from sol-gel-derived thin film made with Ln^{3+}-doped LaF_3 nanoparticles [J]. *J. Am. Chem. Soc.*, 2005, **127**: 12464.

[66] Kido J, Ikeda W, Kimura M, Nagai K. White-light-emitting organic electroluminescent device using lanthanide complexes [J]. *Jpn. J. Appl. Phys. 2, Lett.*, 1996,

35: L394.

[67] Li S, Zhong G, Zhu W H, Li F, Pan J, Huang W, Tian H. Dendritic europium complex as a single dopant for white-light electroluminescent devices [J]. *J. Mater. Chem.*, 2005, **15**: 3221.

[68] Evans C H. Biochemistry of the Lanthanides [M]. New York: Plenum Press, 1990.

[69] Bünzli J C G. Coordination chemistry of the trivalent lanthanide ions : an introductory overview, in Rare Earths [M]. Eds. Puche R Saez and Caro P, Madrid: Editorial Complutense, 1998. 223.

[70] Jr. Horrocks W D, Albin M. Lanthanide ion luminescence in coordination chemistry and biochemistry [J]. *Prog. Inorg. Chem.*, 1984, **31**: 1.

[71] Hemmilä I, Mukkala V M. Time-resolution in fluorometry technologies, labels, and applications in bioanalytical assays [J]. *Crit. Rev. Clin. Lab. Sci.*, 2001, **38**: 441.

[72] Parker D, Williams J A G. Responsive luminescent lanthanide complexes [J]. Metal Ions in Biological Systems. Eds. Sigel A and Sigel H, New York: Marcel Dekker Inc., 2003. 40.

[73] Pandya S, Yu J H, Parker D. Engineering emissive lanthanide complexes for molecular imaging and sensing [J]. *Dalton Trans.*, 2006. 2757.

[74] Johnsson N, Johnsson K. Chemical tools for biomolecular imaging [J]. *ACS Chemical Biology*, 2007, **2**: 31.

[75] Demas J N, Degraff B A. Applications of luminescent transition platinum group metal complexes to sensor technology and molecular probes [J]. *Coord. Chem. Rev.*, 2001, **211**: 317.

[76] Clapp A R, Medintz I L, Mattoussi H. Forster resonance energy transfer investigations using quantum-dot fluorophores [J]. *Chem. Phys. Chem.*, 2006, **7**: 47.

[77] Bazin H, Trinquet E, Mathis G. Time resolved amplification of cryptate emission: a versatile technology to trace biomolecular interactions [J]. *Rev. Mol. Biotechnol.*, 2002, **82**: 233.

[78] Weissleder R, Ntziachristos V. Shedding light onto live molecular targets [J]. *Nature Med.*, 2003, **9**: 123.

[79] Bünzli J-C G. Luminescent Lanthanide Probes as Diagnostic and Therapeutic Tools, in Metal Complexes in Tumor Diagnosis and as Anticancer Agents, Metal Ions in Biological Systems [M]. Eds. Sigel A and Sigel H, New York: Marcel Dekker Inc., 2004, **42**(2): 39.

[80] Mody T D, Fu L, Sessler J L. Texaphyrins: Synthesis and development of a novel class of therapeutic agents [J]. *Prog. Inorg. Chem.*, 2001, **49**: 551.

[81] Gaiduck M I, Grigor'yants V V, Mironov A F, Rumyantseva V D, Chissov V I, Sukhin G M. Fiber-laser IR luminescence diagnostics od malignant tumors using rare-earth porphyrins [J]. *J. Photochem. Photobiol. B Biol.*, 1990, **7**: 15.

[82] Gaiduck M I, Grigoriants V V, Mironov A F, Roitman L D, Chissov V I, Rumiantseva V D, Sukhin G M. IR Luminescence diagnostics of malignant-tumors with the help of metallocomplexes of porphyrins [J]. *Dokl. Acad. Nauk. SSSR*, 1989, **309**: 980.

[83] Chudinov A V, Rumyantseva V D, Lobanov A V,

Chudinova G K, Stomakhin A A, Mironov A F. Synthesis of a water-soluble ytterbium porphyrin-bovine serum albumin conjugate [J]. *Russ. J. Bioorg. Chem. (Engl. Transl.)*, 2004, **30**: 89.

[84] Zijlmans H J M A, Bonnet J, Burton J, Kardos K, Vail T, Niedbala R S, Tanke H J. Detection of cell and tissue surface antigens using up-converting phosphors: A new reporter technology [J]. *Anal. Biochem.*, 1999, **267**: 30.

[85] Boyer J C, Vetrone F, Cuccia L A, Capobianco J A. Synthesis of colloidal upconverting NaYF₄ nanocrystals doped with Er, Yb and Tm, Yb via thermal decomposition of lanthanide trifluoroacetate precursors [J]. *J. Am. Chem. Soc.*, 2006, **128**: 7444.

[86] Raymond K N, Müller G, Matzanke F. Complexation of iron by siderophores. A review of their solution and structural chemistry and biological function [J]. *Top. Curr. Chem.*, 1984, **123**: 49.

[87] Werts M H V, Woudenberg R H, Emmerink P G, van Gassel R, Hofstraat J W, Verhoeven J W. A near-infrared luminescent label based on Yb-III ions and its application in a fluoroimmunoassay [J]. *Angew. Chem. Int. Ed.*, 2000, **39**: 4542.

[88] Zhang J, Badger P D, Greib S J, Petoud S. Sensitization of near-infrared-emitting lanthanide cations in solution by tropolonate ligands [J]. *Angew. Chem. Int. Ed.*, 2005, **44**: 2508.

[89] Comby S, Gumy F, Bünzli J-C G, Saraidarov T, Reisfeld R. Luminescent properties of an Yb podate in sol-gel silica films, solution, and solid state [J]. *Chem. Phys. Lett.*, 2006, **432**: 128.

[90] Comby S, Imbert D, Vandevyver C, Bünzli J-C G. A novel strategy for the design of 8-hydroxyquinolinate-based lanthanide bioprobes emitting in the NIR range [J]. *Chem. Eur. J.*, 2007, **13**: 936.

[91] Bassett A P, Van Deun R, Nockemann P, Glover P B, Kariuki B M, Van Hecke K, Van Meervelt L, Pikramenou Z. Long-lived near-infrared luminescent lanthanide complexes of imidodiphosphinate "Shell" ligands [J]. *Inorg. Chem.*, 2005, **44**: 6140.

[92] Imbert D, Cantuel M, Bünzli J C G, Bernardinelli G, Piguet C. Extending lifetimes of lanthanide-based NIR emitters (Nd, Yb) in the millisecond range through Cr (III) sensitization in discrete bimetallic edifices [J]. *J. Am. Chem. Soc.*, 2003, **125**: 15698.

[93] Torelli S, Imbert D, Cantuel M, Bernardinelli G, Delahaye S, Hauser A, Bünzli J C G, Piguet C. Tuning the decay time of lanthanide-based near infrared luminescence from micro- to milliseconds through d-f energy transfer in discrete heterobimetallic complexes [J]. *Chem. Eur. J*, 2005, **11**: 3228.

[94] Nishioka K, Fukui, K, Matsumoto K. Lanthanide Chelates as Luminescent Labels in Biomedical Analyses [M]. Handbook on the Physics and Chemistry of Rare Earths. Eds. Jr Gschneidner K A, Bünzli J-C G, and Pecharsky V K, Amsterdam: Elsevier Science B.V., 2007. 37.

[95] Nishioka T, Yuan J, Yamamoto Y, Sumitomo K, Wang Z, Hashino K, Hosoya C, Ikawa K, Wang G, Matsumo-

to K. New luminescent europium (III) chelates for DNA labeling [J]. *Inorg. Chem.*, 2006, **45**: 4088.

[96] Picot A, Malvolti F, LeGuennic B, Baldeck P L, Williams J A G, Andraud C, Maury O. Two-photon antenna effect induced in octupolar europium complexes [J]. *Inorg. Chem.*, 2007, **46**: 2659.

[97] Fu L M, Wen X F, Ai X C, Sun Y, Wu Y S, Zhang J P, Wang Y. Efficient two-photon-sensitized luminescence of a europium(III) complex [J]. *Angew. Chem. Int. Ed.*, 2005, **44**: 747.

[98] Scaff W L, Dyer D L, Mori K. Fluorescent europium chelate stain [J]. *Journal of Bacteriology*, 1969, **98**: 246.

[99] Canada R G. Terbium luminescence studies of binding of adriamycin and cisplatin to tumorigenic Cells [J]. *Anal. Chim. Acta*, 1988, **205**: 77.

[100] Phimphivong S, Saavedra R G. Terbium chelate membrane label for time-resolved, total internal reflection fluorescence microscopy of substrate-adherent cells [J]. *Bioconjugate Chem.*, 1998, **9**: 350.

[101] Zohar O, Ikeda M, Shinagawa H, Inoue H, Nakamura H, Elbaum D, Alkon D L, Yoshioka T. Thermal imaging of receptor-activated heat production in single cells [J]. *Biophys. J.*, 1998, **74**: 82.

[102] Manning H C, Goebel T, Thompson R C, Price R R, Lee H, Bornhop D J. Targeted molecular imaging agents for cellular-scale bimodal imaging [J]. *Bioconjugate Chem.*, 2004, **15**: 1488.

[103] Bornhop D J, Griffin J M M, Goebel T S, Sudduth M R, Bell B, Motamedi M. Luminescent lanthanide chelate contrast agents and detection of lesions in the hamster oral cancer model [J]. *Appl. Spectrosc.*, 2003, **57**: 1216.

[104] Bornhop D J, Hubbard D S, Houlne M P, Adair C, Kiefer G E, Pence B C, Morgan D L. Fluorescent tissue site-selective lanthanide chelate, Tb-PCTMB for enhanced imaging of cancer [J]. *Anal. Chem.*, 1999, **71**: 2607.

[105] Hanaoka K, Kikuchi K, Kojima H, Urano Y, Nagano T. Selective detection of zinc ions with novel luminescent lanthanide probes [J]. *Angew. Chem. Int. Ed.*, 2003, **42**: 2996.

[106] Hanaoka K, Kikuchi K, Kojima H, Urano Y, Nagano T. Development of a zinc ion-selective luminescent lanthanide chemosensor for biological applications [J]. *J. Am. Chem. Soc.*, 2004, **126**: 12470.

[107] Parker D. Luminescent lanthanide sensors for pH, pO₂ and selected anions [J]. *Coord. Chem. Rev.*, 2000, **205**: 109.

[108] Pal R, Parker D. A single component ratiometric pH probe with long wavelength excitation of europium emission [J]. *Chem. Commun.*, 2007. 474.

[109] Song B, Wang G, Tan M, Yuan J. A europium(III) complex as an efficient singlet oxygen luminescence probe [J]. *J. Am. Chem. Soc.*, 2006, **128**: 13442.

[110] Jensen T B, Scopelliti R, Bünzli J-C G. Lanthanide triple-stranded helicates: controlling the yield of the heterobimetallic species [J]. *Inorg. Chem.*, 2006, **45**: 7806.

[111] Elhabiri M, Scopelliti R, Bünzli J C G, Piguet C. Lanthanide helicates self-assembled in water: a new class of highly stable and luminescent dimetallic carboxylates[J]. *J. Am. Chem. Soc.*, 1999, **121**: 10747.

[112] Vandevyver C, Chauvin A S, Comby S, Bünzli J-C G. Luminescent lanthanide bimetallic triple-stranded helicates as potential cellular imaging probes [J]. *Chem. Commun.*, 2007, Published on the web, 2007.

[113] Binnemans K, Görller-Walrand C. Lanthanide containing liquid crystals and surfactants[J]. *Chem. Rev.*, 2002, **102**: 2303.

[114] Piguet C, Bünzli J C G, Donnio B, Guillon D. Thermotropic lanthanidomesogens [J]. *Chem. Commun.*, 2006. 3755.

[115] Lunstroot K, Driesen K, Nockemann P, Gorller-Walrand C, Binnemans K, Bellayer S, Le Bideau J, Vioux A. Luminescent ionogels based on europium-doped ionic liquids confined within silica-derived networks [J]. *Chem. Mater.*, 2006, **18**: 5711.

[116] Liu G K, Chen X Y. Spectroscopic properties of lanthanides in nano materials, in Handbook on the Physics and Chemistry of Rare Earths [M]. Eds. Jr. Gschneidner K A, Bünzli J C G, Pecharsky V K, Elsevier Science B.V., Amsterdam, 2007. 37.

[117] Zhang R J, Cui J W, Lu D M, Hou W G. Study on high-efficiency fluorescent microcapsules doped with europium-diketone complex by LbL self-assembly[J]. *Chem. Commun.*, 2007. 1547.

[118] Holsa J, Aitasalo T, Jungner H, Lastusaari M, Niittykoski J, Spano G. Role of defect states in persistent luminescence materials [J]. *J. Alloys Comp.*, 2004, **374**: 56.

[119] Senechal-David K, Hemeryck A, Tancrez N, Toupet L, Williams J A G, Ledoux I, Zyss J, Boucekkine A, Guegan J P, LeBozec H, Maury O. Synthesis, structural studies, theoretical calculations, and linear and nonlinear optical properties of terpyridyl lanthanide complexes: new evidence for the contribution of electrons to the NLO activity [J]. *J. Am. Chem. Soc.*, 2006, **128**: 12243.

[120] Gandara F, Garcia-Cortes A, Cascales C, Gomez-Lor B, Gutierrez-Puebla E, Iglesias M, Monge A, Snejko N. Rare earth arenedisulfonate metal-organic frameworks: an approach toward polyhedral diversity and variety of functional compounds [J]. *Inorg. Chem.*, 2007, Published on the Web, 2007.

[121] Xia J, Zhao B, Wang H S, Shi W, Ma Y, Song H B, Cheng P, Liao D Z, Yan S P. Two- and three-dimensional lanthanide complexes: synthesis, crystal structures, and properties [J]. *Inorg. Chem.*, 2007, Published on the Web, 23, 2007.

[122] Zhu W H, Wang Z M, Gao S. Two 3D porous lanthanide - fumarate-oxalate frameworks exhibiting framework dynamics and luminescent change upon reversible De- and rehydration[J]. *Inorg. Chem.*, 2007, **46**: 1337.